

Ductility and Damage Characteristics of RC Bridge Columns under Cyclic Pure Torsion



Abdeldjelil Belarbi & Qian Li

Department of Civil and Environmental Engineering, University of Houston, USA

SUMMARY:

The presence of torsion affects structural performance of reinforced concrete (RC) bridge columns in terms of strength, deformational capacity and damage limit states such as concrete cracking, reinforcement yielding, and concrete cover spalling, buckling of longitudinal reinforcement and crushing of concrete core. This paper presents an experimental study on five RC columns under reversed cyclic pure torsion with different cross sectional shapes. Cross sectional shape, aspect ratios and transverse reinforcement configurations are considered as variables in this study. Ductility and damage characteristics of these five columns are investigated by comparing torsional hysteresis response, observed damage progression and failure modes with respect to test variables. Additionally, the twist ductility and torsional stiffness characteristics are discussed from a displacement based design point of view. It was found that the torsional ductility, torsional stiffness and damage characteristics were significantly altered with respect to change in cross sectional shape and transverse reinforcement configuration.

Keywords: RC bridge columns; cross sectional shape, cyclic torsion; torsional ductility; damage characteristics

1. GENERAL INSTRUCTIONS

The reinforced concrete (RC) bridge column under significant torsion more likely occurs in skewed or horizontally curved bridges, bridges with unequal spans or column heights, and bridges with outrigger bents. The study on behavior of RC bridge columns subjected to cyclic pure torsion is necessary for generalizing the analysis of columns under combined loading. RC bridge columns under pure torsion behave elastically before concrete cracks; and therefore the cracked members act as a truss where the longitudinal and transverse reinforcement carry most of the tensile force and the resulting concrete strut carries the compressive force. The inclined shear cracks winder spirally around the surface of columns due to the excessive tensile strain in the direction of principal tensile stress. After cracking load, the stress of reinforcement significantly increases up to yielding states and concrete cover starts to spall due to high shear stress in the concrete outside of transverse reinforcement. At higher cycles of loading, torsional plastic hinge forms due to significant concrete cover spalling and severe concrete core degradation. However, the location and distribution of the torsional plastic hinge along the height of columns are different from the flexural one due to different damage and failure mechanisms. Additionally, the rotation and ductility capacity of RC bridge columns become increasingly important according to the seismic design requirement. According to literature review, there have been few experimental studies on pure torsional behavior of RC members (Bishara and Peir, 1973; Pandit and Mawal, 1973; Hsu and Mo, 1985a; Rahal and Collins, 1995a, Koutchoukali and Belarbi, 2001; Browning et al., 2007; Suriya and Belarbi., 2008; Hindi et al., 2011), particularly on torsional damage characteristics, ductility capacity, and stiffness degradation with respect to different cross sectional shape, transverse reinforcement amount and configurations, and aspect ratios. In this experimental study, five RC bridge columns with different cross-sectional shapes, aspect ratios, and transverse reinforcement configurations were tested under cyclic torsional load along with constant axial load. Based on the test results, the torsional moment capacity, ductility, stiffness, energy dissipation, and plastic damage hinge are highlighted and discussed in this paper.

2. EXPERIMENTAL PROGRAM

Specimen Details and Material Properties: In order to investigate the torsional ductility and damage characteristics of RC bridge columns, five half-scale columns with square, circular and oval cross sectional shapes were designed to represent typical bridge columns as shown in Fig. 1. The square column had a width of 550 mm and clear concrete cover of 38 mm. All circular columns had a diameter of 610 mm and clear concrete cover of 25 mm. The oval column was designed with the cross sectional dimension of 610 mm×915 mm. The square and oval columns were designed with an effective height (from the top of footing to the centerline of the applied forces) of 3.35 m. Two of the circular columns were loaded with effective height of 3.66 m; one of them was loaded with effective height of 1.83 m. The aspect ratio was defined as ratio of effective height and cross sectional dimension. For square columns, four No.9 bars (28 mm diameter) and eight No.8 bars (25 mm diameter) were employed as the longitudinal reinforcement to obtain the longitudinal reinforcement ratio of 2.1%. Twelve No.8 bars and twenty No.8 bars were used as longitudinal bars for circular and oval column, respectively, as shown in Fig. 2. Rectangular and octagonal No.3 bar was used as transverse reinforcement for square column with spacing of 83 mm to obtain transverse reinforcement ratio of 1.32%. At the same transverse reinforcement amount level of 1.32%, No.4 (12.7 mm diameter) spirals were used as transverse reinforcement spaced at 70 mm for one of the circular columns and the oval column. To study the transverse reinforcement ratio and configuration effect on torsional behavior, two of the circular columns with high aspect ratio were fabricated with No.3 (9.5 mm diameter) spirals and circular hoop, respectively, at a lower transverse reinforcement ratio of 0.73%. All columns were properly designed to obtain the specific reinforcement ratio and aspect ratio as shown in Fig. 1 and Table 1. Typically, the superstructure dead load induces axial loads in bridge columns varying between 5% and 10% of the capacity of the columns. Therefore, the axial load ratio was taken to be 7% of the concrete capacity of the columns. The concrete was supplied by a local Ready Mix Plant with an expected 28-day design cylinder compressive strength of 34.5 MPa. Deformed bars were used for longitudinal and transverse reinforcement in all columns. Standard tests for concrete compressive strength, modulus of rupture, and tensile tests on steel coupons were conducted to provide accurate material properties. The actual concrete and reinforcement properties of the columns on testing day of columns are given in Table 1.

Experimental Setup and Instrumentation: The axial load was applied by a hydraulic jack on top of the columns to obtain the target 7% axial load ratio. The axial load was measured by a load cell between the hydraulic jack and the top of the load stub. Cyclic torsion was created by imposing equal but opposite directional forces or displacement with the two horizontal servo-controlled hydraulic actuators as shown in Fig. 2. The twist and horizontal displacements of the columns were measured by string transducers at multiple heights above the column footing. Electrical strain gages were attached to the surface of the spirals and transverse reinforcement then mounted at various heights along the whole column.

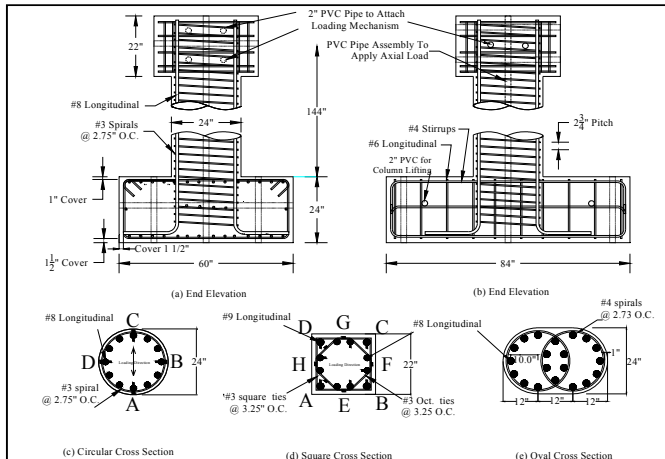


Figure 1. Cross Sectional Details (1 in = 25.4 mm)

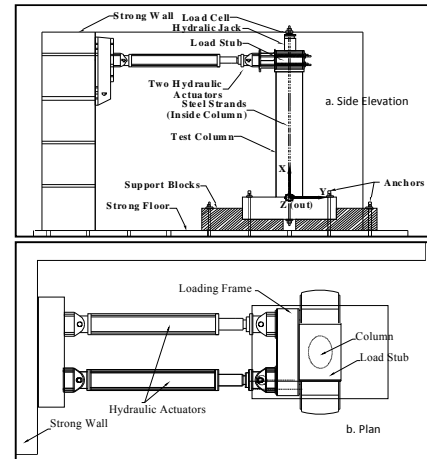


Figure 2. Test Setup

Table 1. Cross Sectional Properties of Concrete and Steel used in Columns

| PROPERTY | Circular (C1) | Circular (C2) | Circular (C3) | Square (S1) | Oval (O1) |
|---|------------------------|------------------------|------------------------|---------------------------|------------------------|
| | H/B(6)-T/M(∞) | H/B(6)-T/M(∞) | H/B(3)-T/M(∞) | H/B(6)-T/M(∞) | H/B(6)-T/M(∞) |
| Transverse Reinforcement Ratio (%) | 0.73 | 0.73 | 1.32 | 1.32 | 1.32 |
| Aspect Ratio (Height/Dimension) | 6 | 6 | 3 | 6 | 5.5 |
| Transverse Reinforcement Configuration | Circular Hoop | Single Spiral | Single Spiral | Square and Octagonal Ties | Interlocking Spirals |
| Compressive Strength (f'_c , MPa) | 25.8 | 37.9 | 28.0 | 34.6 | 32.6 |
| Modulus of Rupture (f_{cr} , MPa) | 2.48 | 3.72 | 3.31 | 3.58 | 3.24 |
| Transverse Reinforcement Yield Strength (ksi) | 462.0 | 462.0 | 462.0 | 472.3 | 472.3 |
| Longitudinal Reinforcement Yield Strength (ksi) | 456.4 | 456.4 | 456.4 | 464.0 | 464.0 |

Loading Protocol: The columns were loaded under cyclic torsion in a load control mode before the yielding load (T_y). The rotation corresponding to yielding load was defined as a twist ductility one ($\mu_0=1$). After the transverse reinforcement yield, the tests were conducted in displacement control mode up to the ultimate failure at high ductility levels. Three loading cycles were applied at each ductility level to provide an indication of stiffness degradation characteristics. For torsional moment, counter-clockwise torque was defined as positive cycles, and that in the clockwise direction as negative cycles.

3. EXPERIMENTAL RESULTS AND DISCUSSION

Circular Column Hysteresis Curves and Observation of Damage Progression: Circular columns with hoop (C1) and spiral (C2) were tested to study the locking and unlocking effect of spiral configuration on hysteresis behavior. Fig. 3 shows the torsional moment-twist hysteresis curve of column C1. Inclined shear cracks occurred around the mid-height of column at 50% of T_y . As the test progressed, the shear cracks lengthened spirally around the column faces with increasing torsional load. The yielding of hoop was observed at torsional moment of 196.7 kN-m and rotation angle of 2.5° , which was considered as ductility level of one. The peak torsional moment was achieved at the ductility level of three when the concrete cover started to spall off. The column obtained the same peak torsional moment in positive and negative cycles indicating no locking and unlocking effect from hoop configurations. The longitudinal bars remained elastic until ductility six and concrete cover spalled off from the 600 mm to 3000 mm height measured from the base of the column. The test was stopped after torsional strength dropped significantly due to core concrete crushing, corresponding to a twist of 18° . Fig. 4 shows the progression of damage at different states.

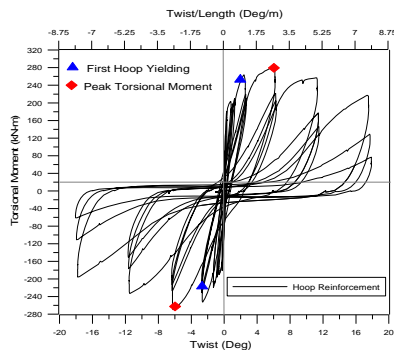


Figure 3. Torsional Hysteresis of Column C1

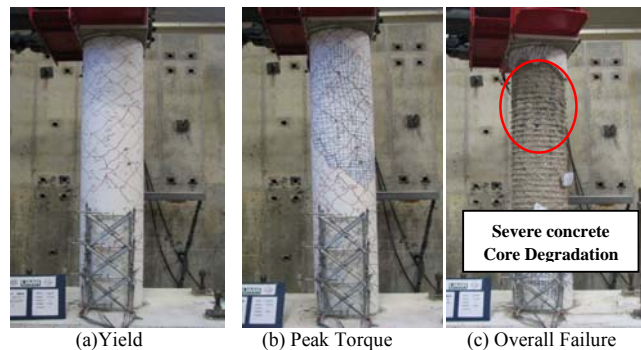


Figure 4. Damage Progression of C1

Fig. 5 shows the torsional moment-twist hysteresis curve of circular column C2. Initial shear cracks were observed during the loading cycle of $0.75T_y$ at the mid-height of the column. Thereafter shear cracks developed with even space in both positive and negative cycles with increasing loading level up to yielding state. The post-cracking torsional stiffness decreased proportionally with an increase in torsional loading. Up to yielding state, severe shear cracks were formed along the full height of the column as shown in Fig. 6 (a). The behavior of circular column with spirals was significantly different from the one with hoops due to the locking and unlocking effects from the spirals. During the positive cycles of torsional loading, more concrete cover spalling and less confinement effect to the concrete core were observed due to the unlocked behavior of spiral reinforcement. During the negative cycles of loading, the spirals were locked with additional confinement contribution to the concrete core. The locking and unlocking effects are reflected in the asymmetric nature of hysteresis curves at post-yielding stage, where the load resistance in negative cycles was higher than that in positive cycles. The spirals reached the yield strain at ductility one; and the longitudinal bars remained elastic until ductility four. Differences in the strain levels were observed on two opposite sides of A and B due to the effect of locking and unlocking of the spirals. Concrete cover spalling started at ductility one and extended to about 80% of the column height at failure state. As compared to column C1, the concrete cover spalled more due to the larger rotational deformation capacity from better confinement of spirals. Significant concrete cover spalling led to the formation of a torsional plastic hinge near mid-height of the column, which contributed to the rotational deformation of the column. After the formation of plastic hinge, dowel action of longitudinal reinforcement acted significantly to resist the load at higher cycles of loading. Concrete core experienced more degradation in the circular column with hoops as compared to the one with spiral because the additional confinement effect of spiral in the locking direction reducing the damage of concrete core as shown in Fig. 6 (c).

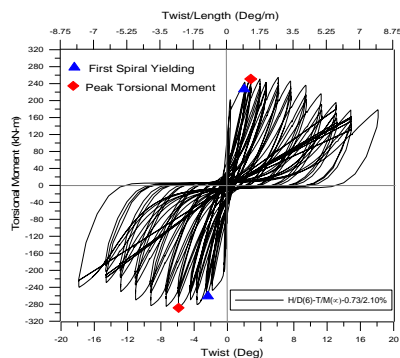


Figure 5. Torsional Hysteresis of Column C2

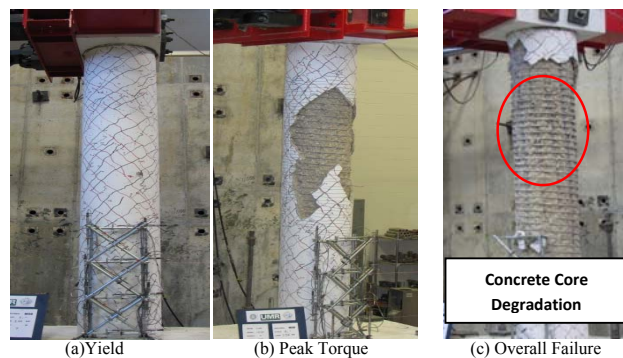


Figure 6. Damage Progression of C2

Fig. 7 shows the torsional hysteresis curve of column C3 with lower aspect ratio and higher transverse reinforcement ratio. For column C3 with lower aspect ratio, larger shear cracks developed near mid-height of the column before the spiral yielded. Soon after yielding state, concrete cover spalling was observed due to severe shear cracks inclined at 44° with respect to the horizontal axis. The even spacing of diagonal shear cracks was larger than other columns due to lower aspect ratio. The locking and unlocking effects of the spirals were also observed in the negative and positive loading cycles at higher ductility levels. Concrete cover spalling continued to develop along the total height of the column at post-yielding state. Then the core concrete crushing developed along the whole column, which is different from localized crushing mode for Columns C1 and C2, due to the more uniform stress distribution along with column comparing to the columns with a high aspect ratio. Based on the comparison, the higher aspect ratio caused severe shear cracks along the whole column and less ductility capacity compared to lower aspect ratio. In addition, no appreciable reduction in torsional strength occurs with a reduction in aspect ratio. Fig. 8 shows the progress on damage of the column C3. An increase in spiral reinforcement ratio provides more torsional resistance and more confinement to concrete core resulting in less degradation of torsional strength and stiffness. Such an increase of transverse reinforcement also improves ductility by increasing deformational capacity and limiting the damage after spirals yielding compared to the one with a lower spiral ratio.

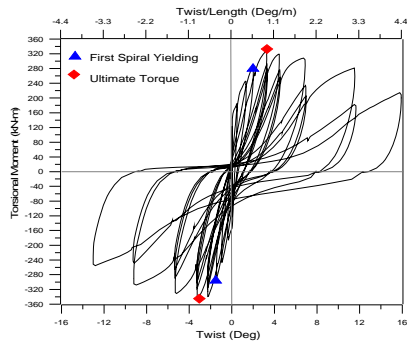


Figure 7. Torsional Hysteresis of Column C3

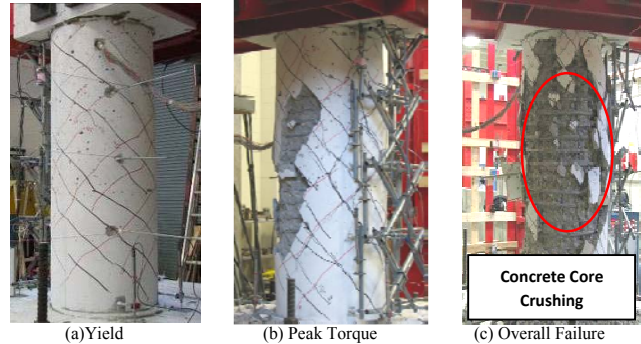


Figure 8. Damage Progression of C3

Square Column Hysteresis Curve and Observation of Damage Procession: In this study, square and octagonal ties were combined as transverse reinforcement for square column to obtain adequate confinement to core concrete and enhance the strength and ductility capacity as spirals configuration. The torsional moment-twist hysteresis response of the column S1 is shown in Fig. 9. The torsional moment is approximately linear up to rotation deformation before cracking and thereafter become nonlinear along with torsional stiffness degradation due to the concrete cracking. The post cracking stiffness decreased proportionally with increasing torsional load and significantly deteriorated after the transverse reinforcement yielded. The inclined shear cracks at approximately 45° occurred near mid-height of column at the load level of $0.6 T_y$. Different from circular columns, the warping effect increased rapidly after torsional cracking load, which results in curved column side faces, severe diagonal crack, and earlier concrete cover spalling. The diagonal shear cracks smeared into core concrete and caused concrete core crushing later at final failure. At post-cracking stage, significant stress developed in transverse and longitudinal reinforcement with increasing load level and the transverse reinforcement around mid-height of column firstly reached its yielding strain at T_y . However, the longitudinal bars on all sides remained elastic until the ductility of 4.5 and then contributed positively to torsional resistance at higher loading level as dowel actions. Concrete cover spalling started at the middle height of column at ductility one and spread to $2/3$ height at ductility eight. Compared to circular columns with spirals, they both experienced severe concrete cover spalling along the whole column. However, the square column was observed with a more localized core concrete damage as compared to circular column due to the concentrated stress at four corners of square column. Also the spiral in circular column resulted in stress redistribution from locking effect to prevent localized core damage. As observed in the test, there is no locking and unlocking effect for the square column. At higher loading cycles, torsional plastic hinge formed near the mid-height of the column due to significant concrete spalling and severe core degradation. Finally, the square and octagonal ties ruptured and longitudinal reinforcement was extremely twisted in the plastic hinge zone leading to the overall failure of the column. Typical damage progress of the column under pure torsion is shown in Fig. 10.

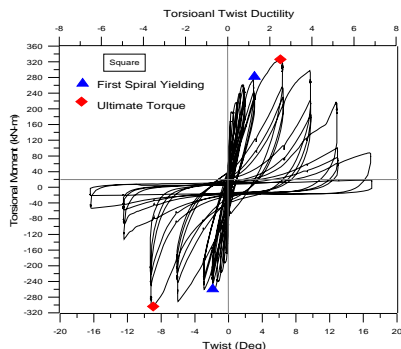


Figure 9. Torsional Hysteresis of Column S1

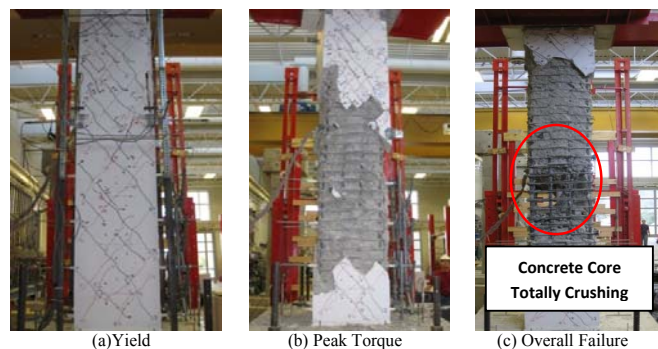


Figure 10. Damage of S1 Column under Pure Torsion

Oval Column Hysteresis Curve and Observation of Damage Procession: The torsional hysteresis

curve of oval column O1 is shown in Fig. 11. The torsional moment-twist curve became nonlinear after the loading level of 50% T_y due to torsional stiffness degradation from concrete cover cracking the same as other columns. Along with increasing load at post-cracking stage, diagonal shear cracks firstly occurred on the straight faces of cross section and then extended along the straight faces due to the warping effect since there is no warping effect on circular curved faces. These shear cracks lengthened and widened with an increase of applied torsion until the yield loading as shown in Fig. 12 (a). Then concrete cover spalling was observed at a ductility level one and the spalling region developed significantly fast to almost 85% before it reached the peak torque at ductility three. Then the concrete cover spalled off the whole column up to ductility six as shown in Fig. 12 (b). This is mainly due to the better confinement from interlocking spirals, which strengthen the core concrete, preventing and lagging the shear cracking to smear into it, and accelerated the concrete cover spalling. Although the cover concrete spalled along the entire length of the column, significant core concrete crushing led to a torsional plastic hinge near higher mid-height of the column as shown in Fig. 12 (c). Fig. 12 indicates the progression of damage in this column with the sequence of shear cracking, concrete cover spalling, spiral yielding, longitudinal bar yielding, and then overall failure by significant core concrete degradation. In addition, the longitudinal bars within the interlocking region transferred the shear stress from spiral to spiral by dowel action of those longitudinal bars which contributed to resist torsional load at high ductility level. The load resistance on the negative cycles was higher than the positive cycles of loading at higher ductility levels due to the different confinement effect caused by the locking and unlocking actions of the double spirals, which is more effective than single spiral.

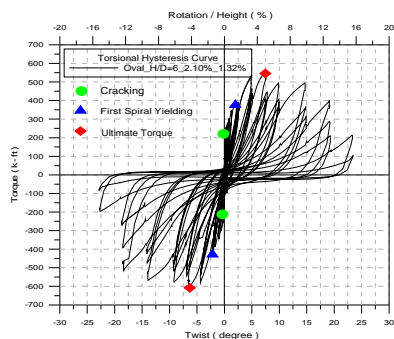


Figure 11. Torsional Hysteresis of Column O1

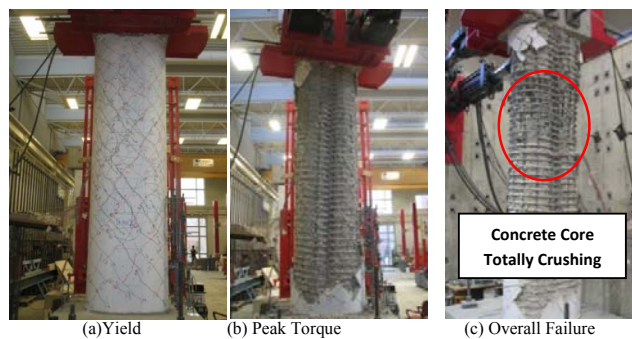


Figure 12. Damage of O1 Column under Pure Torsion

4. TORSIONAL STIFFNESS AND ROTATIONAL DUCTILITY

Torsional stiffness is an important index with respect to load resistance, deformational capacity, and damage limits states for the RC members under cyclic torsion. Secant torsional stiffness is defined as the ratio of torque and corresponding rotation which is used to describe potential torsional resistance. The comparison on secant torsional stiffness of columns is summarized in Fig. 13. Before cracking loading, the torque-twist relationships are not perfect linear because that many minor or micro cracks already happened before the cracking load was monitored and recorded based on the first occurrence of a crack on the outside surface of the column by vision. So the un-cracked torsional stiffness dropped somehow for all the columns as expected, which indicates that even the minor cracks in concrete would reduce the torsional stiffness. Before cracking load, the torsional stiffness mainly depends on the concrete strength, cross sectional shape, and transverse reinforcement configurations but not affected significantly by the amount of reinforcement provided because the reinforcement did not perform actively to torsional resistance before concrete cracking. However, the un-cracked torsional stiffness significantly decreases with an increasing aspect ratio as comparing column C3 to column C1, C2, and S1 respectively, which resulted from the localized concrete cracking pattern for higher aspect ratio; and the column O1 showed higher un-cracked torsional stiffness due to the larger cross-section. In the post-cracking range, the torsional stiffness dropped continuously with more applied loading cycles to a low level when the transverse reinforcement yielded as shown in Fig. 13. Comparison on the torsional stiffness of column S1, O1, and C1 after cracking load validates that increasing the amount of reinforcement increases the cracked torsional stiffness due to more torsional resistance from contribution of transverse reinforcement. For columns with higher aspect ratio of six,

the torsional stiffness decreased to about 20% of cracking torsional stiffness at the yielding stage; while the column C3 with low aspect ratio of three remained larger torsional stiffness at yielding stage, which was about 40% of cracking torsional stiffness. This is also mainly because the columns with a larger aspect ratio experienced a more localized damage pattern resulting in more torsional stiffness degradation and larger rotation. After transverse reinforcement yielded, the secant torsional stiffness was maintained at a low level up to ultimate stage and then decreased to about 5% of cracking torsional stiffness.

Seismic design of RC bridge columns relies on providing a great amount of ductility, which is related to transverse reinforcement ratio, configurations, and lateral confinement. In this study, five columns with different cross-sectional shape and transverse reinforcement configurations were investigated for the torsional ductility characteristics of RC bridge columns. The instant torsional ductility is considered as the ratio of instant rotation to yielding rotation at post-yielding deformational level. The torsional ductility capacity was defined as the ratio of ultimate rotation to yielding rotation, where the ultimate rotation was correspondingly determined based on the ultimate torsional moment (80% of peak torque). The locking and unlocking coefficient was evaluated by the ratio of the difference between positive and negative peak torque to the positive peak torque. The envelopes of torsional moment verses rotation ductility for columns were compared in Fig. 14; and then peak torque, locking and unlocking coefficient, and torsional ductility capacity were summarized in Table 2. Accordingly transverse reinforcement ratio significantly contributed to the torsional moment capacity. However, column C1 with hoops obtained higher peak torque than column C2 with spirals even in the same transverse reinforcement ratio because column C1 were fabricated by concrete with higher strength. So the concrete strength contributed more to the torsional moment capacity than the transverse reinforcement configuration. Also the column O1 obtained the highest torsional moment capacity due to the largest cross sectional area. Though all the columns achieved adequate torsional ductility (usually a ductility of four as required in most design codes), the spirals or interlocking spirals enhanced the torsional ductility capacity and ultimate rotation capacity from the better transverse confinement. In addition, the torsional ductility capacity is not sensitive to the transverse reinforcement ratio when the column was under reinforced. Meanwhile the octagonal and square ties insured square column to achieve the same torsional moment capacity and decent ductility level. But the column C3 with spirals achieved less torsional ductility capacity than other columns with spirals configuration due to the smaller aspect ratio and non-localized failure mode. As compared for the locking and unlocking coefficient, there is no locking and unlocking effect for the columns configured with hoops and ties; while the spirals or interlocking spirals caused obvious locking and unlocking phenomena under cyclic torsional loadings, which should be considered during the RC bridge seismic design. Also, interlocking spirals caused more significant locking and unlocking effect than the single spiral. However, the column C3 with lower aspect ratio behaved less locking and unlocking effect than the column C2 with higher aspect ratio even though it had larger spiral ratio, which indicated that slender columns with large aspect ratio magnified more locking and unlocking effect.

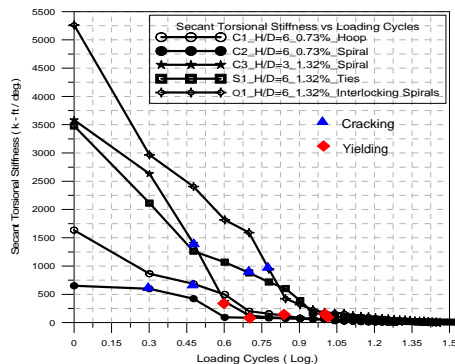


Figure 13. Torsional Stiffness of Columns

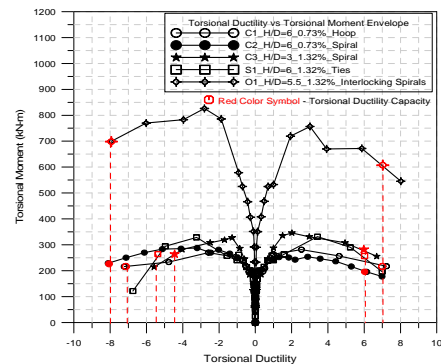


Figure 14. Torsional Ductility of Columns

Table 2. Comparison of Peak Torque, Locking & Unlocking Coefficient and Ductility Capacity

| Columns | C1 | | C2 | | C3 | | S1 | | O1 | |
|-----------------------------------|-----------------------|-----|-----------------------|-----|-----------------------|-----|------------------------------|-----|------------------------|-----|
| Transverse Reinforcement | Circular Hoop (0.73%) | | Single Spiral (0.73%) | | Single Spiral (1.32%) | | Square and Oct. Ties (1.32%) | | Double Spirals (1.32%) | |
| Aspect Ratio | H/D=6 | | H/D=6 | | H/D=3 | | H/D=6 | | H/D=5.5 | |
| Peak Torque (kN-m) | + | - | + | - | + | - | + | - | + | - |
| | 203 | 201 | 187 | 212 | 241 | 255 | 244 | 242 | 557 | 756 |
| Locking and Unlocking Coefficient | 0.00098 | | 0.134 | | 0.058 | | 0.00082 | | 0.357 | |
| Torsional Ductility Capacity | 7 | | 8 | | 6 | | 6 | | 8 | |

5 TORSIONAL DAMAGE CHARACTERISTICS AND DISTRIBUTION

The observed sequence of damage under cyclic torsional moment in this study can be categorized as follows: (i) shear cracking, (ii) transverse reinforcement yielding, (iii) severe shear crack and concrete cover debonding, (iv) spalling of cover concrete, (v) longitudinal reinforcement yielding, (vi) crushing of core concrete, and (vii) longitudinal reinforcement extremely twist or buckling. Diagonal shear cracks will occur in concrete cover when the principal tensile stress reaches the tensile strength of concrete. For columns under torsional loadings, diagonal shear cracks firstly occurred around the mid-height of the column and then developed up and down parallel with even spacing along the overall height of columns. The cracks developed normal to the direction of principal tensile stress and inclined at around 45° direction with respect to longitudinal axis as typically shown in Fig. 15 (a). After concrete cracking, the transverse reinforcement will be highly strained to yield with increasing torsional load which is a signal of the onset of permanent structural distress and an important damage limit state from a torsional ductility point of view since it is a remark of ductile performance. All the columns yielded at the similar rotation angle range from 2.2°-2.8°. At post-yielding stage, the shear cracks lengthened, widened and smeared further deeply into the inner cross section. Thereafter severe shear cracks causes the concrete cover debonding off the transverse reinforcement and core concrete, which results in significant torsional stiffness degradation and indicates the onset of concrete cover spalling. The concrete cover spalling represents moderate damage within desirable repair ranges as typically shown in Fig. 15 (b). The distribution of concrete cover spalling along the columns height definitely affects the serviceability requirements and plays an important role in seismic design and analysis, since it determines the effective cross section area and confinement length to core concrete provided by transverse reinforcement. At a larger loading level, the longitudinal bar achieved yielding stage due to the fact that torsional loads induce uniform levels of tensile strain in the longitudinal bars. Successive progress of longitudinal bar yielding happened over the cross section due to geometric property. It was found that the yielding starts on the corner bars and gradually spreads to adjacent bars around the column circumference for square (S1) and oval (O1) columns; while the yielding starts randomly for the circular columns. The strain development in longitudinal reinforcement confirms the contribution of them to torsional resistance at higher torsional loading level. After the principle stress in core concrete reaches the compressive strength of concrete, the crushing starts in the diagonal

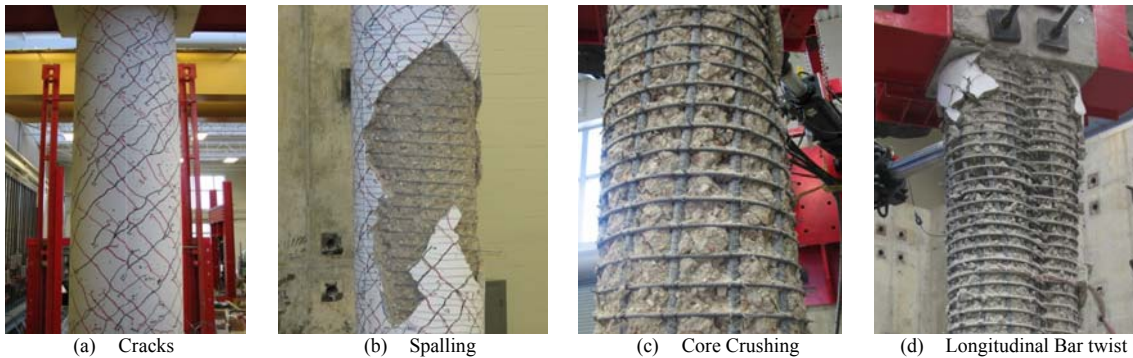


Figure 15. Typical Torsional Damage Characteristic States

concrete strut followed by extremely core concrete degradation as typically shown in Fig. 15 (c). After severe concrete cover spalling and significant degradation of concrete core, the transverse and longitudinal reinforcement were exposed without effective cover by concrete, which caused longitudinal bars to extremely rotate and then buckle as typically shown in Fig. 15 (d). Extreme twisting and buckling of longitudinal bars was observed in the torsional plastic damage zone for all columns. Moreover, the concrete cover spalling under torsional loads is influenced by the cover and lateral dimension ratio, the axial load ratio, and the aspect ratio. The concrete cover spalling and damage zone distribution along the height of the columns were compared in Fig. 16, which indicated that the length of concrete cover spalling corresponded to almost the full length of columns except column C3 because they are designed with a similar axial load ratio, aspect ratio, and cover lateral dimension ratio, and loaded under uniform torsion along the full length. However, the column C3 achieved less concrete spalling length compared to other columns due to the lower aspect ratio. It is also found that the concrete spalling length is affected by transverse reinforcement ratio based on the comparison on column C1, C2, S1 and O1. The length and location of plastic damage zone are summarized in Table 3. For column C1, C2, S1, and O1 with higher aspect ratio, they were all observed with a damage zone length around 1.2 times of the cross section dimension, which is 18% to 20% of the total length of the column. However, the column C3 with lower aspect ratio achieved a larger damage zone length around 50% of the total length of the column, which concluded that the columns with high aspect ratio behaved more localized failure; while the column with low aspect ratio was more likely to fail in non-localized mode. The severe core crushing zone for columns with spirals or interlocking spirals located at approximate 65% ~68% of the total column height, which contributed most to the rotation capacity. However, column S1 obtained the severe core crushing at the right mid-height of the column (around 53%). Hence, the shape of cross section and transverse reinforcement configuration play an important role in the distribution of plastic damage zone. Additionally column S1 experienced more severe core concrete crushing than other columns with spirals because of the less effective confinement to core concrete provided from ties.

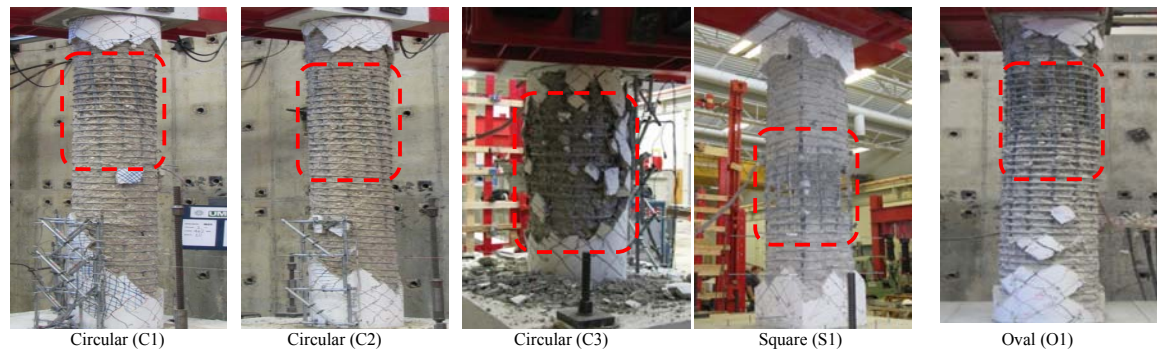


Figure 16. Concrete Spalling and Damage Zone Distribution

Table 3. Comparison of Damage Zone Location and Length

| Column | C1 | C2 | C3 | S1 | O1 |
|--------------------------------------|-----------------------|-----------------------|-----------------------|------------------------------|------------------------|
| Transverse Reinforcement | Circular Hoop (0.73%) | Single Spiral (0.73%) | Single Spiral (1.32%) | Square and Oct. Ties (1.32%) | Double Spirals (1.32%) |
| Aspect Ratio | H/D=6 | H/D=6 | H/D=3 | H/D=6 | H/D=5.5 |
| Damage Zone Length (mm) | 650 | 660 | 790 | 600 | 685 |
| Damage Zone Length/Column Length (%) | 19.4 | 19.7 | 47.1 | 17.9 | 20.4 |
| Damage Zone Location (mm From Base) | 2286 | 2159 | 838 | 1776 | 2275 |

4. SUMMARY

This study conducted experiments on five RC columns under reversed cyclic torsion, and the following concluding remarks can be drawn:

- 1) The failure of RC bridge columns under pure torsion was initiated by reinforcement yielding, severe diagonal cracking of concrete and concrete cover spalling and finalized by formation of core concrete crushing near the mid-height of the column. In addition, dowel action of longitudinal bars contributed significantly to the load resistance at higher cycles of torsional loading.
- 2) Before cracking load, the torsional stiffness is mainly affected by concrete strength and cross sectional shape but not by the amount of reinforcement. Torsional stiffness significantly decreases with an increase in aspect ratio; while the increasing amount of reinforcement increases the cracked torsional stiffness. In addition, the columns with larger aspect ratio experienced more localized damage pattern resulting in more torsional stiffness degradation.
- 3) The concrete cover spalling distribution is sensitive to aspect ratio. The column C3 with lower aspect ratio experienced less concrete cover spalling than other ones with larger aspect ratios. The concrete spalling length is not significantly affected by the transverse reinforcement ratio based on the comparison on column C1, C2, S1, and O1.
- 4) The location and length of the torsional damage zone alters mainly depending on the cross sectional shape, transverse reinforcement configuration, and aspect ratio. Columns with higher aspect ratio reached smaller damage zone length around 18% to 20% of the total length of the column. However, the columns with lower aspect ratio achieved a larger damage zone length, around 50% of the total length of specimen, which concludes that the columns with high aspect ratio behaved more localized failure.
- 5) The spirals or interlocking spirals enhanced the torsional ductility capacity and ultimate rotation. The octagonal and square ties helped the square column to achieve the target torsional moment capacity and decent ductility level. In addition, the torsional ductility capacity was not affected by the transverse reinforcement ratio for the under reinforced columns. But it degraded along with the decrease in aspect ratios due to the non-localized failure mode.
- 6) There is no locking and unlocking effect for the columns configured with hoops and ties; while the spirals or interlocking spirals caused obvious locking and unlocking phenomena under cyclic torsional loading. Furthermore, large aspect ratio can magnify locking and unlocking effect.

REFERENCE

- Bishara, A. and Peir, J.C. (1973). Reinforced Concrete Rectangular Columns in Torsion. *Journal of Structural Division* **94: ST 12**, 1409-1421.
- Browning, B., Marvel, L. and Hindi, R. (2007). Torsional Ductility of Circular Concrete Bridge Columns. *ASCE Structures Congress 2007*,
- Hindi, Riyadh A. and Browning Benjamin J. (2011). Torsionally Loaded Circular Concrete Members Confined with Spirals. *ACI Structural Journal* **98:4**, 139-147.
- Hsu, T. T. C. and Mo. Y. L. (1985). Softening of Concrete in Torsional Members – Theory and Tests. *ACI Structural Journal* **82:3**, 290-303.
- Koutchoukali, N. E. and Belarbi, A. (2001). Torsion of High-Strength Reinforced Concrete Beams and Minimum Reinforcement Requirement. *ACI Structural Journal* **98:4**, 462-469.
- Pandit, G.S. and Mawal, M.B. (1973). Tests of Concrete Columns in Torsion. *Journal of Structural Division* **99:ST7**, 1409-1421.
- Rahal, K.N. and Collins, M.P. (1995). Effect of the Thickness of Concrete Cover on the Shear-Torsion Interaction – an Experimental Investigation. *ACI Structural Journal* **92:3**, 334-342.
- Prakash, S. and Belarbi, A. (2010). Towards Damage Based Design Approach for RC Bridge Columns under Combined Loadings Using Damage Index Models. *Journal of Earthquake Engineering* **14:3**, 363-389.